Quantification of Excluded Volume Effects on the Folding Landscape of *Pseudomonas aeruginosa* Apoazurin *In Vitro*

Alexander Christiansen and Pernilla Wittung-Stafshede*
Department of Chemistry, Umeå University, Umeå, Sweden

ABSTRACT Proteins fold and function inside cells that are crowded with macromolecules. Here, we address the role of the resulting excluded volume effects by in vitro spectroscopic studies of *Pseudomonas aeruginosa* apoazurin stability (thermal and chemical perturbations) and folding kinetics (chemical perturbation) as a function of increasing levels of crowding agents dextran (sizes 20, 40, and 70 kDa) and Ficoll 70. We find that excluded volume theory derived by Minton quantitatively captures the experimental effects when crowding agents are modeled as arrays of rods. This finding demonstrates that synthetic crowding agents are useful for studies of excluded volume effects. Moreover, thermal and chemical perturbations result in free energy effects by the presence of crowding agents that are identical, which shows that the unfolded state is energetically the same regardless of method of unfolding. This also underscores the two-state approximation for apoazurin's unfolding reaction and suggests that thermal and chemical unfolding experiments can be used in an interchangeable way. Finally, we observe increased folding speed and invariant unfolding speed for apoazurin in the presence of macromolecular crowding agents, a result that points to unfolded-state perturbations. Although the absolute magnitude of excluded volume effects on apoazurin is only on the order of 1–3 kJ/mol, differences of this scale may be biologically significant.

INTRODUCTION

To function, proteins must fold from extended unfolded states to compact unique structures that are biologically active. Through pioneering work during the last three decades, significant progress has been made to pinpoint mechanisms and driving forces important for protein folding. However, in reality, proteins fold inside cells where the environment is very different from the dilute buffer solutions mostly used in in vitro experiments. The intracellular environment is highly crowded due to the presence of large amounts of macromolecules, including proteins, nucleic acids, ribosomes, and carbohydrates. This means that a significant fraction of the intracellular space is not available to other macromolecular species. It has been estimated that the concentration of macromolecules in the cytoplasm ranges from 80 to 400 mg/ml (1,2). All macromolecules in physiological fluids collectively occupy between 10% and 40% of the total aqua-based volume (3). The crowded environment results in excluded volume effects, risk of nonspecific intermolecular interactions, and increased bulk viscosity.

Minton coined the word macromolecular crowding in 1981 (4) to address the impact of volume exclusion from macromolecules (5–7). Due to excluded volume effects, any reaction resulting in a volume change will be affected by macromolecular crowding (5,8). Therefore, macromolecular crowding will provide a stabilizing effect to the folded states of proteins indirectly due to destabilization of the more extended and malleable denatured states (9,10). It has been predicted (5,11,12) and shown in vitro (13,14) that the unfolded ensemble becomes more compact in crowded conditions. The effects of excluded volume on the activity of protein folded and unfolded states, thereby also on overall protein stability, have been predicted by Minton (5,11,15) using a statistical thermodynamic approach (16) involving the hard particle model for solutions of rigid macromolecules (17) and scaled particle theory (18,19) to obtain closed equations. In the simplest models, the folded and unfolded states are mimicked as effective hard spheres of appropriate sizes and the crowding molecule as a solid sphere (19,20) or solid rod (21). In subsequent work, the modeling of the unfolded ensemble was made more realistic by taking into account Monte Carlo simulations (22) and using a Gaussian cloud model with intramolecular steric repulsion (5). Although these models give predictions of crowding effects that can be tested in vitro, few such validations have been successfully executed.

To create excluded volume conditions in vitro, one may use so-called macromolecular crowding agents that are inert, noncharged polymers of defined sizes (i.e., dextrans, Ficoll) that occupy space but do not interact with target proteins (7,23,24). Ficoll 70 is a sucrose-based polymer, whereas dextrans are glucose-based polymers that are available in various sizes. Several in vitro experiments have shown that protein stability and folding speed can be affected by the presence of macromolecular crowding agents (6,10,25–29). However, often these experiments are hampered by irreversibility and aggregation in the presence of crowding agents, limiting thermodynamic analysis. In some recent studies, (inert) proteins have been used as the crowding agent (instead of sugar polymers) with the idea that this is a more in vivo-like scenario. In these experiments, in addition to technical issues arising when dealing

Submitted June 20, 2013, and accepted for publication August 15, 2013.

*Correspondence: pernilla.wittung@chem.umu.se

Editor: Patricia Clark.

0006-3495/13/10/1689/11 $2.00

http://dx.doi.org/10.1016/j.bpj.2013.08.038

with very high concentrations of proteins and the limitations of useful detection methods, often electrostatic interactions were observed and the target protein was not always stabilized in the presence of another protein in high amounts (30,31). Nonspecific electrostatic interactions are expected for high concentrations of charged macromolecules (or if very low salt concentration) and it was concluded early on that, in such cases, electrostatic effects may counteract (if electrostatic attraction) or strengthen (if electrostatic repulsion) the excluded volume effect (15,32). A few studies of protein folding in vivo (33–35) have shown that the importance of nonspecific electrostatic effects, in relation to excluded volume effects, may depend on the choice of target protein and what cellular compartment is analyzed.

In addition to excluded volume effects (and electrostatic interactions if charged molecules), the bulk viscosity of crowded solutions will increase. This phenomenon is more a hydrodynamic effect and should not affect equilibrium positions and structures, but may slow down folding kinetics if the rate-limiting folding step is controlled by diffusion. If not diffusion controlled, the magnitude of crowding effects on folding kinetics will depend on the relative sizes of the folded, unfolded, and transition states (for a simple two-state folder). One should bear in mind that albeit the bulk viscosity is dramatically increased, crowded solutions are heterogeneous and the microviscosity the polypeptide is experiencing during its folding reaction is likely only increased two- to threefold (36–38).

Our approach to understanding protein biophysics in vivo is to assess individual contributions one by one in vitro. Here, we present a methodical study of the folding energy landscape (thermal and chemical stability, as well as folding dynamics) of a model protein as a function crowding agent identity, size, and amount. We choose the well-characterized 14 kDa protein, *Pseudomonas aeruginosa* apoazurin (*Inset*, Fig. 1) as the model system because it folds in two-state equilibrium and kinetic processes and most of the reactions are reversible in the presence of crowding agents. We find that thermally and chemically induced changes in apoazurin stability due to the presence of crowding agents can be modeled by the simple excluded volume theory. In accord with a compact folding-transition state, the crowding effects can be explained exclusively by unfolded-state perturbations.

MATERIALS AND METHODS

Chemicals

Sodium phosphate (NaP), Ficoll 70, and guanidine hydrochloride (GuHCl) were from Sigma-Aldrich, St. Louis, MO. Technical grade Dextrans 20, 40 and 70 were from Pharmacosmos, Holbaek,Denmark. GuHCl and crowding agents were prepared as stock solutions in 20 mM NaP at pH 7.0. The GuHCl concentration was determined by refractive index (Abbe refractometer). The concentrations of crowder stocks were determined by angle of rotation (Kruess polarimeter, Hamburg, Germany).

Protein purification

Pseudomonas aeruginosa apoazurin was expressed in *Escherichia coli* and purified as described (39). In brief, the periplasmic preparation was purified by cation-exchange and gel filtration on an AKTA instrument (Pharmacia, Uppsala, Sweden). Fractions containing azurin were dialyzed against 0.5 M potassium cyanide (KCN) to remove copper and zinc (Zn), followed by dialysis into 20 mM NaP pH 7.0. Presence of Zn-bound azurin was determined by $CuSO_2$ titration; it corresponded to <5% of the total protein. Protein concentration was determined by absorption (ε_{280} = 8605 $M^{-1}cm^{-1}$).

Equilibrium unfolding

Thermal unfolding experiments of apoazurin at different crowder concentrations were performed on a Jasco-720 circular dichroism (CD)-spectrophotometer connected to a peltier element in a 1-mm cell. The change in CD signal at 220 nm (2 nm bandwidth, 4 s integration time) was followed as a function of temperature (20°C to 85°C). Two scan rates were used (0.5 and 1.0 deg/min). The protein concentration in the measurements varied between 10 and 20 μM.

GuHCl-induced unfolding was detected by fluorescence changes at 310 nm (excitation 285 nm, 5 nm excitation, and emission slid widths, 3 mm path length) on a Cary Eclipse fluorimeter. The temperature was kept at 20°C with a peltier element. 25 or more individual protein samples of different GuHCl concentrations were prepared for each crowder concentration. The samples were incubated for 1 h before measurement and allowed to equilibrate in the instrument for 15 min before measurement. The final protein concentration varied between 5 and 10 μM.

Time-resolved folding/unfolding

Apoazurin refolding and unfolding kinetics were measured on an Applied Photophysics Chirascan stopped-flow instrument in a 2-mm cell. Unfolding was triggered by mixing protein in buffer with a solution containing a high concentration of GuHCl; refolding was achieved by diluting apoazurin that was unfolded in 2.5 M GuHCl with a solution of buffer. The reaction was followed by CD at 220 nm and total fluorescence (305 nm cutoff filter, 5 nm bandwidth, 285 nm excitation) with an interval of 0.01 s. The mixing ratio was 1:10 with a final protein concentration of 14 μM. The temperature was kept at 20°C with a water bath. The dead time in the mixing experiments was dependent on the presence of crowder: dead time of 2.7 ms in buffer but 5.8 ms in the presence of 200 mg/ml Dextran 20.

Experimental data analysis

Chemically and thermally induced unfolding reactions of apoazurin were analyzed using a two-state model involving folded (F) und unfolded (U) states: U ↔ F. The associated equilibrium constant for unfolding (K_U) is defined as the ratio of fraction unfolded over fraction folded and the associated change in free energy is $\Delta G_U = -R \times T \times \ln(K_U)$. Observed spectroscopic signals (Y_{obs}) in the unfolding reactions were fitted to Eq. 1:

$$Y_{obs} = (Y_U + m_U \times X - (Y_F + m_F \times X)) \times \frac{\exp(-\Delta G_U(X)/RT)}{(1+\exp(-\Delta G_U(X)/RT))} + (Y_F + m_f \times X), \quad (1)$$

where Y_F/Y_U and m_F/m_U stand for folded/unfolded signal and slope of the baseline, respectively. X is temperature or concentration of GuHCl depending on the mode of denaturation (thermal versus chemical). In the case of

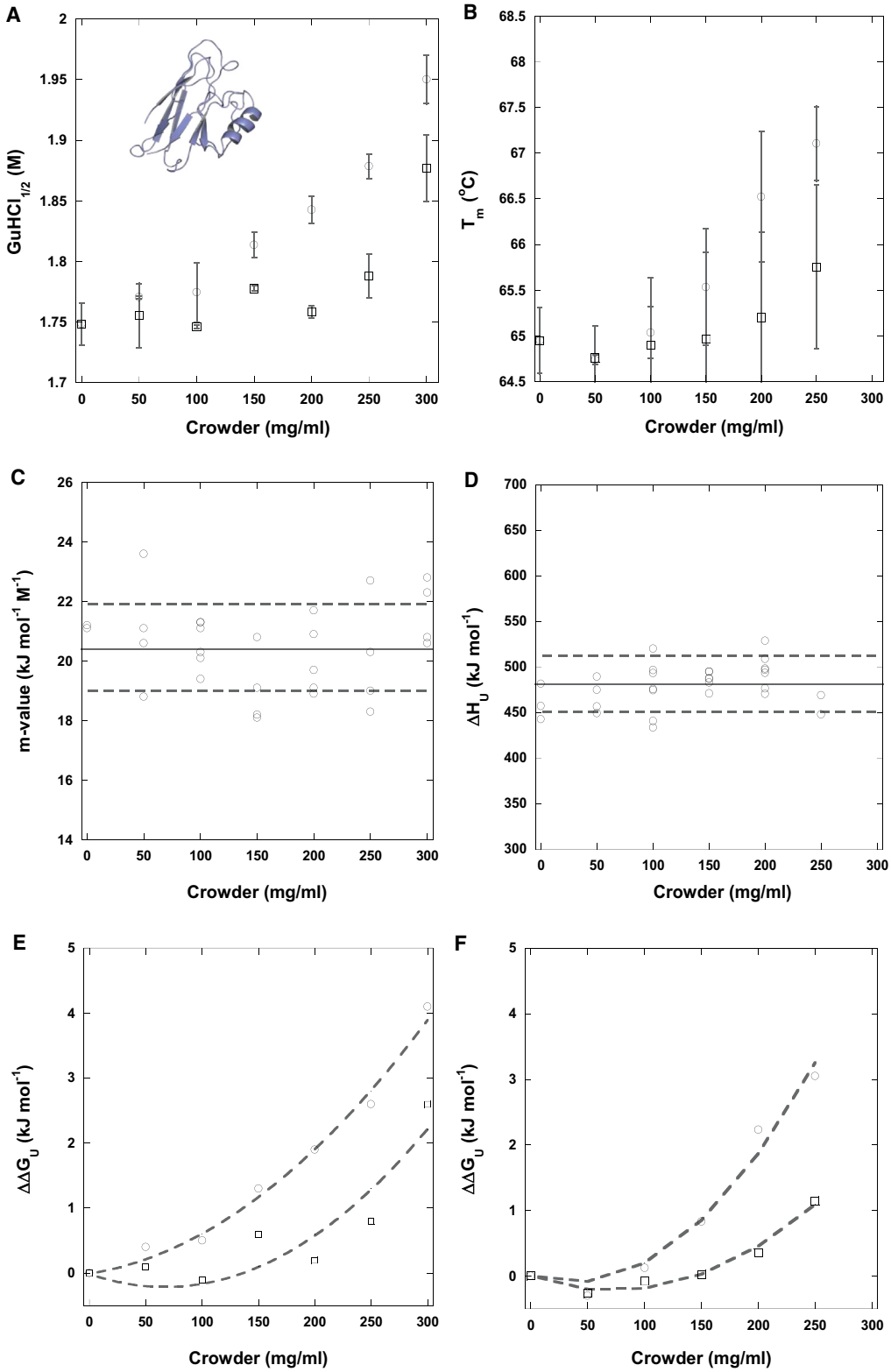

FIGURE 1 Midpoints of chemically induced (*A*) and thermally induced (*B*) unfolding reactions of apoazurin in the presence of various concentrations of Dextran 20 (*circles*) and Ficoll 70 (*squares*). The error bars represent the standard deviation of the mean from two (Dextran 20) or three (Ficoll 70) individual measurements in *A*, and 3–5 individual measurements in *B*. Inset in *A* shows a cartoon of the structure of *P. aeruginosa* apoazurin. In *C* and *D*, the m-values and ΔH_U values for chemically induced and thermally induced unfolding, respectively, are plotted as a function of crowder concentration. In each plot, the solid line is the average value and the broken lines correspond to one standard deviation. *E* and *F* show the calculated $\Delta\Delta G_U$ values (i.e., $\Delta G_{U,crowd}$-$\Delta G_{U,buffer}$) from chemically induced (*E*) at 20°C and thermally induced (*F*) at 65°C unfolding reactions. The broken lines represent the best quadratic fit to the data. To see this figure in color, go online.

GuHCl-induced unfolding, a linear dependence of ΔG_U(GuHCl) with GuHCl concentration was assumed (40,41):

$$\Delta G_U(\mathrm{GuHCl}) = \Delta G_U(H_2O) + m \times [\mathrm{GuHCl}], \quad (2)$$

where m reports on the cooperativity of the transition and/or solvent exposure upon unfolding (42) and $\Delta G_U(H_2O)$ is the unfolding free energy extrapolated to 0 M GuHCl. The data for GuHCl-induced unfolding was fitted without sloping baselines. For thermal unfolding, ΔG_U at the midpoint temperature of unfolding (T_m) is zero and because $\Delta G_U = \Delta H_U - T \times \Delta S_U$, at T_m $\Delta H_U(T_m)$ is equal to $T_m \times \Delta S_U(T_m)$. Assuming ΔH_U and ΔS_U to be constant around T_m, i.e., setting Δc_p to be zero in a small temperature range around T_m, gives the following expression that can be used to replace $\Delta G_U(X)$ in Eq. 1:

$$\Delta G_U = \Delta H_U - T \times \frac{\Delta H_U}{T_m}. \quad (3)$$

This results in Eq. 4, which was used to fit thermal unfolding data directly:

$$Y_{obs} = \frac{(Y_U + m_U \times T - (Y_F + m_F \times T)) \times (\exp(-\Delta H_U/RT) \times (1 - T/T_m))}{(1 + \exp(-\Delta H_U/RT) \times (1 - T/T_m))} + (Y_F + m_F \times T). \quad (4)$$

The kinetic traces for apoazurin refolding were fitted with a double exponential decay function and for unfolding with a single exponential decay function. This is in agreement with previous reports of apoazurin folding kinetics (43–46). For refolding, only the major (>90% of amplitude) phase was used for analysis.

Theoretical analysis

For the F ↔ U transition, the associated equilibrium constant in dilute buffer is $K_{U,buffer}$ and the activity coefficient γ is assumed to be 1. In the presence of crowders, the solution is clearly nonideal, and the F ↔ U transition is affected because the activity coefficients for folded and unfolded states diverge (increase) from 1. The equilibrium constant at crowded conditions, $K_{U,crowd}$, corresponds to $K_{u,buffer} \times (\gamma_F/\gamma_U)$ where γ_U is larger than γ_F because the unfolded state is larger in size than the folded state (5,11,20). Therefore, the crowding effect on protein stability, $\Delta\Delta G_U = \Delta G_{U,crowd}$-$\Delta G_{U,buffer}$, (which we can determine experimentally) is equal to $RT \times \ln\gamma_F$-$RT \times \ln\gamma_U$.

To compare experimental $\Delta\Delta G_U$ data for apoazurin to theoretical predictions of excluded volume effects on stability, we used scaled particle theory involving two-body steric interactions in which the crowding agent was represented as an array of rods (20,21), in analogy with the approach used in (6). The crowding effect on protein stability can then be predicted according to Eq. 5 assuming spherical representations of folded and unfolded states:

$$\Delta\Delta G_U = \left(\left(1 + \frac{r_U}{r_C}\right)^2 - \left(1 + \frac{r_F}{r_C}\right)^2\right) v_C \times w_C \times RT, \quad (5)$$

where r_F and r_U are the hard sphere radii of folded and unfolded protein states; r_C is the cylinder radius of a rod-shaped crowder and w_C is the concentration of crowder in g/l. Note that this equation only represents scenarios where the crowding rods are much longer than the protein dimensions. For the crowder partial specific volume (v_C), we have used 0.65 ml/g for both dextran and Ficoll, which is an experimental value determined by us previously (27). The hard sphere radius, $r_{U/F}$, in Eq. 5 can be related to the radius of gyration, R_G, (as used in e.g., (5)), which is a measurable parameter:

$$r = \sqrt{\left(\frac{5}{3}\right)} \times R_G. \quad (6)$$

RESULTS

Apo-azurin unfolds in a two-state equilibrium reaction (44–47) that can be probed by far-UV CD and tryptophan fluorescence (Fig. S1 in the Supporting Material). The $\Delta G_U(H_2O)$ at 20°C is 36 kJ/mol with midpoint at 1.75 M GuHCl, and T_m in buffer is 65°C at our conditions.

In Fig. 1, *A* and *B*, we show the effects on the chemically induced unfolding midpoint (at 20°C) as well as on the thermal unfolding midpoint (T_m) in the presence of increasing amounts of macromolecular crowding agents (0–300 mg/ml; increments of 50 mg/ml). Independent of the method of perturbation (chemical or thermal), addition of increasing the amount of crowding agent leads to an increase in the midpoint of unfolding (Fig. 1, *A* and *B*). The cooperativity of the unfolding transitions (m-value in chemical unfolding and ΔH_U in thermal unfolding) on the other hand does not change systematically upon the addition of crowder (Fig. 1, *C* and *D*). For further analysis we used the average m-value (20.4 kJ $mol^{-1}M^{-1}$) and ΔH_U (481 kJ mol^{-1}). All data parameters are summarized in Table S1.

The reversibility of apoazurin unfolding was at least 90% in thermal experiments in buffer, and for all crowder conditions in the GuHCl experiments. However, presence of crowding agents in concentrations above 200 mg/ml resulted in decreased recovery of refolded protein in the thermal experiments due to high-temperature aggregation. Nonetheless, we did not detect any dependence of T_m on scan rate or protein concentration, in accord with an irreversible process occurring after the thermal transition.

The $\Delta\Delta G_U(H_2O)$ values (=$\Delta G_U(H_2O,crowder)$-$\Delta G_U(H_2O,buffer)$) determined by chemical unfolding at 20°C and $\Delta\Delta G_U$(338K) values (=ΔG_U(338K,crowder)-ΔG_U(338 K,buffer)) from thermal unfolding as a function of the crowding agent concentration are shown in Fig. 1, *E* and *F*. The $\Delta\Delta G_U$ values from thermal experiments were calculated using the van't Hoff equation and the average ΔH_U value extrapolating from $T_{m,crowd}$ for each condition to $T_{m,buffer}$. Neglecting Δc_p in these short extrapolations is acceptable because inclusion of a Δc_p contribution in the

calculations would add <0.3 kJ/mol to $\Delta\Delta G_U$. From Fig. 1 *E* and *F*, it appears that the dependence of $\Delta\Delta G_U$ with crowder concentration is nonlinear. An f-test for a linear and quadratic model gave a statistical significance of the quadratic model ($\alpha = 0.05$). The nonlinearity is dictated by the >200 mg/ml of crowder data points. An f-test omitting 250 and 300 mg/ml data points gives no improvement by adding a quadratic term, i.e., a linear model is sufficient to explain the dependence of $\Delta\Delta G_U$ on crowding agent concentration up to 200 mg/ml Dextran/Ficoll.

To assess the influence of crowder-size on protein stability, thermal and chemical unfolding experiments of apoazurin in the presence of Dextran 70 and Dextran 40 were performed. The results were compared to the data for Dextran 20 and are listed in Table 1 and shown graphically in Fig. S2. It is evident that for the same concentration of crowder (in mg/ml), the size of the dextran (at least in the range 20–70 kDa) does not matter for its effect on apoazurin stability. Thus, the crowding effect of dextran is independent of the size of the dextran. In accord with our finding, no dextran-size effect was noted in a previous report (28). However, in another report, the authors concluded that a dextran-size dependence was present, although the effects observed were weak (48).

Pairwise comparisons of $\Delta\Delta G_U$ values from thermal and chemical unfolding experiments for all of the Dextran 20 and Ficoll 70 concentrations (Fig. 2) show that both modes of denaturation result in similar effects on $\Delta\Delta G_U$. In accord with an excluded volume effect that is entropy based, this correlation also suggests that the magnitude of the crowding effect is independent of temperature (chemical stability values obtained at 20°C; thermal stability values are for 65°C).

Next, to reveal how the crowding-induced stability effects are divided into folding- and unfolding-rate constants, we compared apoazurin folding dynamics in buffer with that in the presence of various amounts of Dextran 20, as a function of GuHCl concentration at 20°C. We selected Dextran 20 because it has the lowest viscosity of the dextrans and this property allows for kinetic studies at higher concentrations. Because there was no dextran-size dependence in the equilibrium stability data, we reasoned that kinetic data with dextran of one particular size would be representative for dextrans of all sizes. Concentrations up to 200 mg/ml were chosen because they are within the linear regime of the thermal/chemical stability data. Folding and unfolding reactions of apoazurin remain single-exponential in the presence of Dextran 20, like in buffer, at all crowding/denaturant conditions. Moreover, at all GuHCl conditions

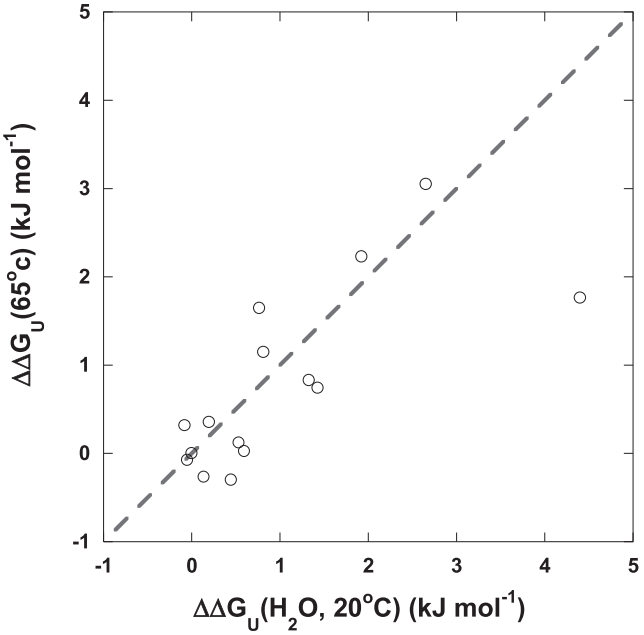

FIGURE 2 Pairwise comparisons of $\Delta\Delta G_U$ values obtained from chemical unfolding at 20°C (*x* axis) and from thermal unfolding at 65°C (*y* axis) for each particular crowder condition. The broken line corresponds to a perfect match between the two values.

TABLE 1 GuHCl-induced unfolding-transition midpoints ($D_{1/2}$ in M GuHCl) and m-values obtained from fitting of GuHCl-induced unfolding transitions at 20°C (pH 7) in the presence of different concentrations and sizes of Dextrans as indicated

Crowder	Amount (mg ml^{-1})	$D_{1/2}$ (M)[a]	m-value (kJ mol^{-1} M^{-1})[a]	$\Delta G_U(H_2O)$ (kJ mol^{-1})[b]	T_m (°C)[a]
Dextran 20	100	1.77 (±0.01)	20.8 (±1.0)	36.3 (±1.5)	65.0 (±0.3)
Dextran 70	100	1.75 (±0.02)	20.4 (±0.5)	35.8 (±1.6)	65.6 (±0.4)
Dextran20	200	1.84 (±0.01)	19.4 (±0.5)	37.7 (±1.6)	66.5 (±0.7)
Dextran 40	200	1.82	21.3	37.3 (±1.6)	66.4 (±0.9)
Dextran 70	200	1.80 (±0.03)	19.7 (±3.5)	36.9 (±1.7)	68.1 (±0.5)
Dextran 20	250	1.89 (±0.01)	18.7 (±0.5)	38.7 (±1.6)	67.1 (±0.4)
Dextran 40	250	1.93	17.0	39.6 (±1.6)	–
Dextran 70	250	1.93	15.3	39.6 (±1.6)	–
Dextran 20	300	1.96 (±0.02)	20.4 (±0.3)	40.2 (±1.7)	–
Dextran 40	300	1.96	19.5	40.2 (±1.7)	–
Dextran 70	300	1.96	19.5	40.2 (±1.7)	–

Lack of thermal data (–) is due to protein aggregation upon unfolding.

[a]The errors in parenthesis are from comparisons of at least two repetitions. The fitting errors in each fit are $<\pm 0.005$ M for $D_{1/2}$ values and <1.0 kJ mol^{-1} M^{-1} for the m-values.

[b]ΔG_U was calculated according to $\Delta G_U = D_{1/2} \times m$ using an average m-value (20.4 kJ mol^{-1}).

far-UV CD and fluorescence detection methods gave the same kinetic result, in support of a two-state process (Fig. S3). The resulting Chevron plots (ln k_{obs} vs. [GuHCl]) for apoazurin folding/unfolding kinetics without and with 200 mg/ml Dextran 20 are shown in Fig. 3 *A*. In the transition region, 1.5–2.5 M, the arms of the Chevron plot are linear, whereas at lower GuHCl concentrations downward curvature is apparent. Folding/unfolding kinetic parameters for the linear range are summarized in Table S2. Inspection of the data reveals that with Dextran 20 the folding speed of apoazurin is increased, whereas the unfolding rate constants are unaffected. We also compared the effects of increasing amounts of Dextran 20 (in 50 mg/ml increments between 0 and 200 mg/ml) on the apoazurin refolding/unfolding rate constants at six different GuHCl concentrations (Fig. 3 *B*). From the data it is clear that the refolding rate constants increase linearly with crowding in this interval and there is no effect on apoazurin unfolding speed at any crowder concentration below 200 mg/ml.

The changes in folding rate constants due to crowding could be converted into free-energy effects, i.e., $\Delta\Delta G_U$, via $RT \times \ln(k_{f,crowd}/k_{f,buffer})$ because the unfolding rate constants were unaltered upon additions of the crowding agent. The free-energy effects for apoazurin due to increasing concentrations of dextran 20 are plotted as a function of crowder concentration in Fig. 4. We note that the $\Delta\Delta G_U$ values from the kinetic experiments at three different GuHCl concentrations are identical at each individual crowder concentration, and the values have comparable magnitudes as in the corresponding equilibrium unfolding experiments. This observation shows that the magnitude of the crowding effect on apoazurin free energy is not dependent on the GuHCl concentration or, in other words, does not depend on initial protein stability.

The $\Delta\Delta G_U$ values from chemical unfolding were fitted to an excluded volume model in which the folded (F) and unfolded (U) states are represented as hard spheres and Ficoll and Dextran as an array of cylindrical rods of different diameters. Using our data (up to 200 mg/ml in Fig. 1 *C*) we fitted it to Eq. 5, using $R_{G,F}$ of 16 Å (49) for folded azurin, $v_c = 0.65$ ml/g (27) and $r_C = 7$ Å for Dextran (50) and 14 Å for Ficoll (51) as input values to obtain an estimate for r_U and thereby $R_{G,U}$. The best fits to the data give $R_{G,U}$ of 19.5 ± 0.4 Å for the Dextran 20 data set and 18.3 ± 1.0 Å for the Ficoll 70 data set (Fig. 5). These $R_{G,U}$ values are within errors of each other (~19 Å) and thus show that with the same parameters, both dextran and Ficoll data can be captured by the simple excluded volume theory. A small value of $R_{G,U}$ (but still larger than $R_{G,F}$) for unfolded apoazurin is expected because it contains a disulfide bridge, connecting residue 3 and 26, which is not broken upon unfolding. For lysozyme, which has a similar size as azurin and contains several disulfide bridges, $R_{G,U}$ is around 20 Å (52).

DISCUSSION

Several factors arising from the crowded environment will affect protein biophysical properties in vivo as compared to in dilute buffer solutions. If one wants to know a protein's absolute stability in vivo, one may try to assess this by experiments in vivo; however, if one wants to know why the protein has certain stability in vivo, one has to dissect individual contributions in a controlled manner. Volume

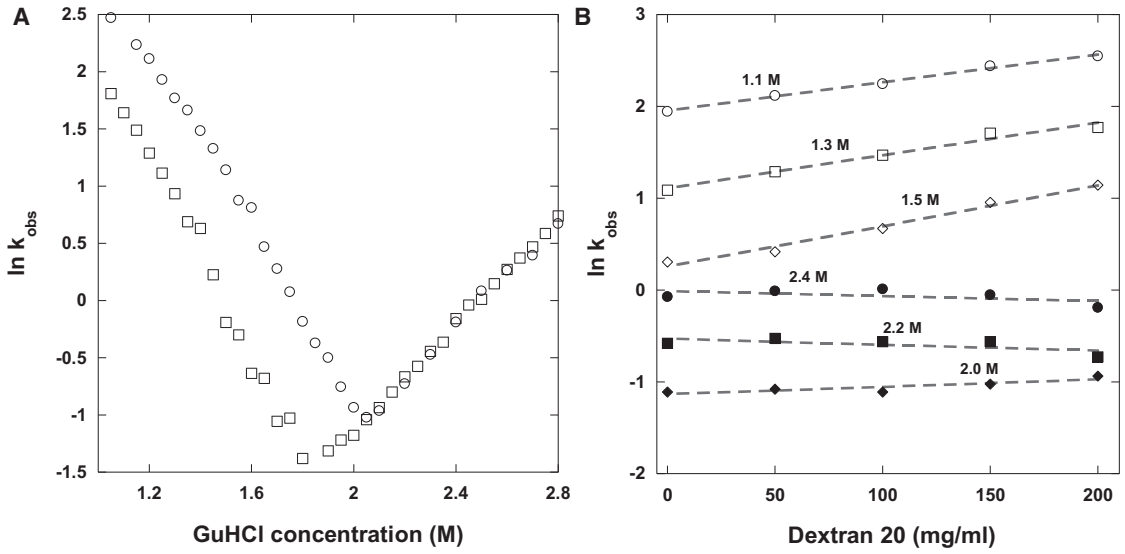

FIGURE 3 Folding/unfolding kinetics of apoazurin in the presence and absence of Dextran 20. (*A*) Chevron plot ($\ln k_{obs}$ versus GuHCl concentration) without (*squares*) and with (*circles*) 200 mg/ml Dextran 20. (*B*) $\ln k_{obs}$ as a function of 50 mg/ml increments of Dextran 20 for three GuHCl concentrations in the folding arm (1.1 M, 1.3 M, and 1.5 M) and three concentrations in the unfolding arm (2.0 M, 2.2 M, and 2.4 M) as indicated in the figure. The broken lines are linear fits to the data points.

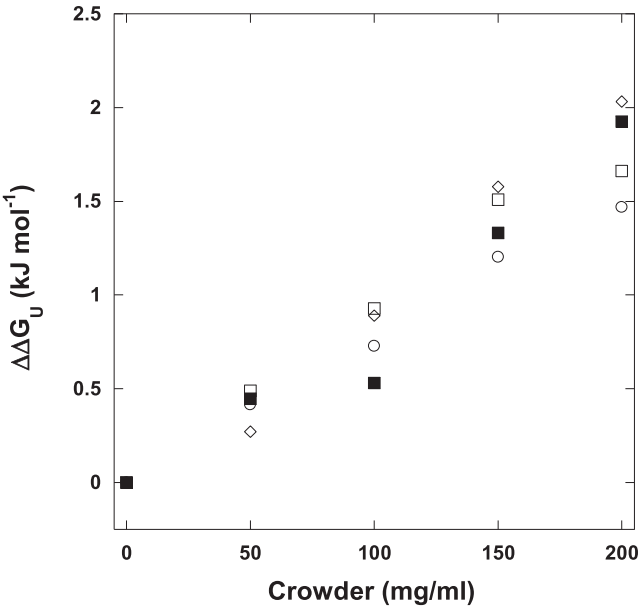

FIGURE 4 $\Delta\Delta G_U$ calculated as RT × $\ln(k_{f,crowd}/k_{f,buffer})$ for the three different GuHCl concentrations studied in Fig. 3 *B* (1.1, 1.3, 1.5 M) is plotted as a function of crowder concentration (*circles*, 1.1 M; *squares*, 1.3 M; *diamonds*, 1.5 M) and, for comparison, $\Delta\Delta G_U$ from equilibrium unfolding experiments (Fig. 1 *E*) is also shown (*solid squares*).

exclusion in cellular environments is an unavoidable phenomenon and, depending on net charge of the macromolecules, electrostatic interactions may tune the overall effect

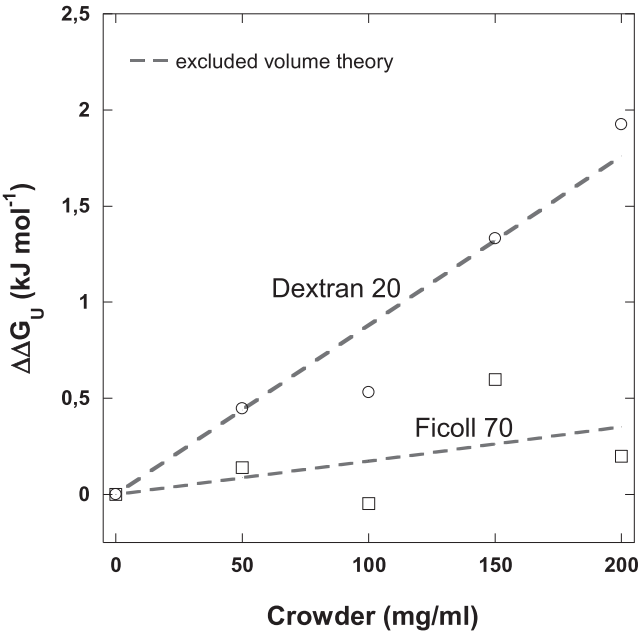

FIGURE 5 The excluded volume model for rod crowders (Eq. 5) was fitted to the $\Delta\Delta G_U$ values from chemical unfolding for Dextran 20 and Ficoll 70 (Fig. 1 *E*). The broken lines are the best fit of Eq. 5 to the experimental data (excluding 250 and 300 mg/ml data points) with $R_{G,U}$ floating (see text for details). For Ficoll 70 (*squares*) a crowder cylindrical radius of 14 Å was used and for Dextran 20 (*circles*) a crowder cylindrical radius of 7 Å was used.

in both directions. It is important to remember that cells are heterogeneous such that concentrations and identity of macromolecules (as well as of small solutes) may fluctuate both temporally and spatially (53). Here, we have quantified excluded volume effects on protein folding and stability in vitro using noncharged synthetic crowding agents (bulk viscosities for the crowding agents are reported in Table S3) and a simple two-state folding protein, apoazurin. Our experimental data have been compared to theoretical predictions of excluded volume effects.

Starting with the statistical mechanics solution theory, Minton derived equations for the two-body interaction/viral coefficient that are based on hard particle modeling of macromolecules. It is assumed that the two-body viral coefficient captures most of the nonideality of the solution and that this term stems from steric interactions only (i.e., no electrostatic effects). Importantly, experimental data support these assumptions for many nonideal protein systems (15). Minton then used the Lebowitz scaled particle theory for hard sphere crowders (19) and Ogston's available volume theory for rod-shaped crowders (21) to derive equations for excluded volume effects on protein stability and conformation. Furthermore, instead of simply treating the unfolded state of the target protein as a solid sphere of an appropriate size, he developed models for random coil ensembles that were based on Brownian and self-avoiding walks (11) as well as the more realistic Gaussian cloud model (5) and calculated the average unfolded-state dimension over a distribution of nonnative conformational states in the presence of crowders. Regardless of using the more sophisticated model or the simple equivalent hard sphere model of the unfolded state, the results in terms of thermodynamic and structural effects by crowders were similar. This suggested that to capture excluded volume phenomena, simple hard particle assumptions (appropriate spheres for folded and unfolded states, and rod or sphere for the crowding molecule) are sufficient under many conditions. Whereas the two-body viral coefficient for nonideal solutions is easily derived, higher order viral coefficients are much more complex and analytical solutions are not available.

Inspection of our data show that upon treating folded and unfolded states as effective hard spheres and dextran as a hard rod (much longer than the dimensions of the protein) with cylindrical radius 7 Å (50) and Ficoll 70 as a rod with cylindrical radius 14 Å (51), excluded volume effects on apoazurin stability are predicted that are in quantitative agreement with the experimental results, at least up to 200 mg/ml (Fig. 5). As predicted by this model, the effect on apoazurin stability by Ficoll 70 is less than that by the different dextrans. This trend arises from the thicker cylindrical dimension, r_C, used to model Ficoll 70, as compared to dextran, in equation 5. As also predicted by this theoretical model, we find no dextran-size dependence in the experimental stability effects (Table 1, Fig. S2). Because pure

excluded volume interactions are entropic in nature, they should not affect enthalpic contributions to protein stability. Our findings of constant ΔH (thermal unfolding) and constant m-value (chemical unfolding) as a function of crowder concentration (Fig. 1, *C* and *D*), support the presence of only excluded volume interactions in our protein-crowder mixtures.

The equation for the effect on protein stability by excluded volume interactions by hard rods predicts a linear dependence on crowder concentration in mg/ml. The experimental data however deviates from linearity at high amounts of the crowding agents (>200 mg/ml) (see Fig. 1, *E* and *F*). We speculate that at these conditions, higher order viral coefficients (i.e., three-body interactions and higher) cannot be neglected and such additional factors would scale nonlinear with the crowder concentration. Also in (11) was a nonlinear dependence on $\Delta\Delta G_U$ predicted theoretically at crowding agent concentrations higher than 200 mg/ml. The issue of nonlinearity has been addressed for experimental values of osmotic pressure of proteins and it was found that up to 100 mg/ml of crowding agent, the two-body term is sufficient to explain the data, whereas when concentrations approach and pass 200 mg/ml of crowding agents, the three-body term started to play a role (32). From a technical point of view, the polymer solutions will approach the concentrated regime, i.e., where they start to behave as monomers instead of macromolecules, at polymers concentrations above 300 mg/ml.

Early work suggested Ficoll 70 to be a semirigid sphere with a radius of ~5 nm (23). In Fig. S4, we show the predicted excluded volume effect on apoazurin stability for a 5-nm sphere. When using the experimentally determined partial specific volume for Ficoll 70, 0.65 ml/g, to obtain the fraction occupied volume at different mg/ml of Ficoll, the predicted effects match the experimental data and, furthermore, there is an upward curvature in both prediction and experimental data. However, a solid sphere of 5 nm with a molecular weight of 70,000 (mass of Ficoll 70) would result in an unrealistically high partial specific volume of ~5 ml/g. In contrast, the experimental value for the specific volume for Ficoll 70 would correspond to a solid sphere with a very small radius (only 2.3 nm). The predicted effect on apoazurin stability when the crowder is a 2.3-nm sphere is also shown in Fig. S4. Thus, although the solid-sphere equation can be used to match the experimental data, the simple arguments above related to partial specific volumes indicate that this analysis is not appropriate. The report of Ficoll 70 being a sphere with a radius of 5 nm likely corresponds to a loosely packed structure, which may be better modeled as a spherocylindrical rod, as suggested by Minton (51) and used in our analysis.

Folding of apoazurin in buffer occurs on the ms timescale (44,46,54,55). The folding transition state of apoazurin has been found via phi-value analysis to be native-like with several fully formed interactions in the core (46,47,55). In parallel, the Tanford β-value, that defines the position of the transition state reaction coordinate relative to that of unfolded (defined as 0) and folded (defines as 1) state coordinates, is 0.67 for apoazurin (46,47,55). Here, we collected kinetic data for apoazurin folding/unfolding dynamics as a function of GuHCl without and with 200 mg/ml dextran 20. Inspection of the full Chevron plots reveals a tendency for folding-arm curvature in both data sets (Fig. 3 *A*). This appearance was earlier described for zinc-substituted azurin with the explanation of a moving transition state (55). To avoid the curvature region, here we analyzed the data between 1.4 M and 2.6 M GuHCl (Table S2) and also performed direct comparisons at specific GuHCl concentrations where data had been collected (Fig. 3 *B*). We find that whereas folding rate constants are increased in the presence of dextran 20, in a crowder-concentration dependent linear fashion, unfolding rate constants are unperturbed by the presence of dextran 20. The simplest explanation for this result is that the presence of crowding agents affect the free energy of the unfolded state, as predicted by simple crowding theory, but has little and similar effects on folded and transition states. This reasoning is fully compatible with the native-like transition state structure demonstrated for apoazurin previously, and also demonstrated here via the high Tanford β-value (Table S2). Recent kinetic folding and unfolding experiments on cytochrome b_{562} in the presence of 85 mg/ml PEG 20 (56,57), and on the Lyme disease protein, VlsE, in the presence of 100 mg/ml Ficoll 70 (25), also show macromolecular crowding effects on the folding-rate constants (rates become faster), but no effects on the unfolding-rate constants.

Large effects due to the presence of macromolecular crowding have been observed for processes such as DNA replication, DNA transcription, amyloid aggregation, virus assembly, and protein oligomerization (58–60): all are reactions involving large changes in volume. In contrast, the absolute effects of macromolecular crowding on protein equilibrium stability and folding kinetics are often found to be smaller (58,61). Here, we find approximately two- to threefold increases in K_{eq} and k_f (at 200 mg/ml dextran 20) for apoazurin in the presence of the crowding agent as compared to in dilute buffer. This magnitude of the crowding effect is reasonable because the volume changes involved in protein folded-unfolded transitions are not as large as for reactions such as protein aggregation, virus assembly and protein oligomerization. Existing in vitro experimental data for the effects of the presence of macromolecular crowding agents on protein stability (T_m and ΔG_U) are summarized in a recent review (62). The available data is sparse in terms of the number of such studies reported (16 T_m and ΔG_U entries reported in (62)). Moreover, most often each study is accomplished with one particular crowding agent at one particular concentration and, thus, no concentration-dependent trends are investigated. Although it is unreliable to draw general

conclusions, it is evident that in most reported cases, the magnitude of the crowding effect on protein stability is comparable to that reported here for apoazurin (6,25–29,56). Nevertheless, because protein concentrations and activities are tightly regulated in vivo, small changes in protein equilibrium and kinetic properties may decide between the life and death of cells. It was recently shown that small changes in kinetic and equilibrium parameters for one particular enzyme resulted in large consequences on organism fitness (63). For example, less than a twofold change in the K_m for the tetracycline resistance protein toward the antibiotics minocylin resulted in a 250% increase in cell growth rate. Moreover, there is a correlation between instability of the tumor suppressor protein p53 and cancer (64). p53 has marginal stability and small decreases in its stability (such as by mutation) may result in unfolding and decreased cellular p53 levels; this may in turn allow for the development of cancer. For cooperative systems, i.e., O_2 binding to hemoglobin, small changes in affinity may have dramatic effects on activity and has been linked to several diseases (65). It appears that the crowded cell environment, due to excluded volume effects, adds an extra bit of stability to all proteins and, for marginally stable proteins, this can be a difference between folded (life) and unfolded (death) states. Moreover, deliberate changes in cellular crowdedness may be a way for organisms to modulate enzyme reactivity and binding affinity.

CONCLUSIONS

At least five conclusions can be drawn from the current work. First, the simple excluded volume theory using hard sphere models for folded and unfolded states, and rod models for the crowding agents, quantitatively captures the experimental effects on apoazurin's thermodynamic stability by additions of dextrans and Ficoll 70. This finding shows that synthetic crowding agents are useful for studies of excluded volume effects and that they should be modeled as rods. Second, there is no dextran-size dependence for the apoazurin stability effects by the different dextrans studied (20, 40, and 70 kDa). This is in accord with the rod model, as it assumes rods of infinite length. However, this result also emphasizes that crowder-size dependence on protein properties cannot be studied using dextrans of different sizes. Third, the match between equilibrium and kinetic effects on apoazurin by the presence of dextran 20 suggest that the expected increase in microviscosity due to the crowders do not slow down apoazurin's folding speed. The increase in folding speed and invariant unfolding speed found for apoazurin in the presence of crowding agents point to unfolded-state perturbations (as predicted by theory (5,11,12) and shown in vitro for a few cases (13,14)). Fourth, thermal and chemical unfolding experiments give the same result in the presence of crowders (when converted to free energy), which shows that the unfolded state is energetically the same regardless of method of unfolding. This underscores the two-state approximation for apoazurin's unfolding reaction and further suggests that thermal and chemical unfolding experiments can be used in an interchangeable way. Finally, although the absolute magnitude of excluded volume effects on apoazurin's folding landscape (and for many other small monomeric proteins) is not particularly impressive (1–3 kJ/mol), differences of this magnitude may be decisive in vivo.

SUPPORTING MATERIAL

Three tables and four figures are available at http://www.biophysj.org/biophysj/supplemental/S0006-3495(13)00985-5.

We thank Allen Minton, Margaret Cheung, and Magnus Wolf-Watz for helpful discussions of data analysis.

The Swedish Natural Research Council, the Knut and Alice Wallenberg Foundation, Göran Gustafsson Foundation, and Umeå University provided financial support.

REFERENCES

1. Zimmerman, S. B., and S. O. Trach. 1991. Estimation of macromolecule concentrations and excluded volume effects for the cytoplasm of *Escherichia coli*. *J. Mol. Biol.* 222:599–620.
2. Rivas, G., F. Ferrone, and J. Herzfeld. 2004. Life in a crowded world. *EMBO Rep.* 5:23–27.
3. Ellis, R. J., and A. P. Minton. 2003. Cell biology: join the crowd. *Nature.* 425:27–28.
4. Minton, A. P. 1981. Excluded volume as a determinant of macromolecular structure and reactivity. *Biopolymers.* 20:2093–2120.
5. Minton, A. P. 2005. Models for excluded volume interaction between an unfolded protein and rigid macromolecular cosolutes: macromolecular crowding and protein stability revisited. *Biophys. J.* 88:971–985.
6. Sasahara, K., P. McPhie, and A. P. Minton. 2003. Effect of dextran on protein stability and conformation attributed to macromolecular crowding. *J. Mol. Biol.* 326:1227–1237.
7. Zhou, H. X., G. Rivas, and A. P. Minton. 2008. Macromolecular crowding and confinement: biochemical, biophysical, and potential physiological consequences. *Annu. Rev. Biophys.* 37:375–397.
8. Laurent, T. C., and A. G. Ogston. 1963. The interaction between polysaccharides and other macromolecules. 4. The osmotic pressure of mixtures of serum albumin and hyaluronic acid. *Biochem. J.* 89:249–253.
9. Zhou, H. X. 2004. Loops, linkages, rings, catenanes, cages, and crowders: entropy-based strategies for stabilizing proteins. *Acc. Chem. Res.* 37:123–130.
10. Cheung, M. S., D. Klimov, and D. Thirumalai. 2005. Molecular crowding enhances native state stability and refolding rates of globular proteins. *Proc. Natl. Acad. Sci. USA.* 102:4753–4758.
11. Minton, A. P. 2000. Effect of a concentrated "inert" macromolecular cosolute on the stability of a globular protein with respect to denaturation by heat and by chaotropes: a statistical-thermodynamic model. *Biophys. J.* 78:101–109.
12. Mittal, J., and R. B. Best. 2010. Dependence of protein folding stability and dynamics on the density and composition of macromolecular crowders. *Biophys. J.* 98:315–320.
13. Mikaelsson, T., J. Åden, …, P. Wittung-Stafshede. 2013. Direct observation of protein unfolded state compaction in the presence of macromolecular crowding. *Biophys. J.* 104:694–704.

14. Hong, J., and L. M. Gierasch. 2010. Macromolecular crowding remodels the energy landscape of a protein by favoring a more compact unfolded state. *J. Am. Chem. Soc.* 132:10445–10452.

15. Minton, A. P. 1998. Molecular crowding: analysis of effects of high concentrations of inert cosolutes on biochemical equilibria and rates in terms of volume exclusion. *Methods Enzymol.* 295:127–149.

16. McMillan, W. G., and J. E. Mayer. 1945. The statistical thermodynamics of multicomponent systems. *J. Chem. Phys.* 13:276–305.

17. Ross, P. D., and A. P. Minton. 1977. Analysis of non-ideal behavior in concentrated hemoglobin solutions. *J. Mol. Biol.* 112:437–452.

18. Boublik, T. 1974. Statistical thermodynamics of convex molecule fluids. *Mol. Phys.* 27:1415–1427.

19. Lebowitz, J. L., E. Helfand, and E. Praestgaard. 1965. Scaled particle theory of fluid mixtures. *J. Chem. Phys.* 43:774–779.

20. Minton, A. P. 1983. The effect of volume occupancy upon the thermodynamic activity of proteins: some biochemical consequences. *Mol. Cell. Biochem.* 55:119–140.

21. Ogston, A. G. 1970. On the interaction of solute molecules with porous networks. *J. Phys. Chem.* 74:668–669.

22. Goldenberg, D. P. 2003. Computational simulation of the statistical properties of unfolded proteins. *J. Mol. Biol.* 326:1615–1633.

23. Venturoli, D., and B. Rippe. 2005. Ficoll and dextran vs. globular proteins as probes for testing glomerular permselectivity: effects of molecular size, shape, charge, and deformability. *Am. J. Physiol. Renal Physiol.* 288:F605–F613.

24. Bohrer, M. P., G. D. Patterson, and P. J. Carroll. 1984. Hindered diffusion of dextran and ficoll in microporous membranes. *Macromolecules.* 17:1170–1173.

25. Homouz, D., M. Perham, …, P. Wittung-Stafshede. 2008. Crowded, cell-like environment induces shape changes in aspherical protein. *Proc. Natl. Acad. Sci. USA.* 105:11754–11759.

26. Stagg, L., S. Q. Zhang, …, P. Wittung-Stafshede. 2007. Molecular crowding enhances native structure and stability of alpha/beta protein flavodoxin. *Proc. Natl. Acad. Sci. USA.* 104:18976–18981.

27. Christiansen, A., Q. Wang, …, P. Wittung-Stafshede. 2010. Factors defining effects of macromolecular crowding on protein stability: an in vitro/in silico case study using cytochrome *c*. *Biochemistry.* 49:6519–6530.

28. Waegele, M. M., and F. Gai. 2011. Power-law dependence of the melting temperature of ubiquitin on the volume fraction of macromolecular crowders. *J. Chem. Phys.* 134:095104.

29. Stagg, L., A. Christiansen, and P. Wittung-Stafshede. 2011. Macromolecular crowding tunes folding landscape of parallel α/β protein, apoflavodoxin. *J. Am. Chem. Soc.* 133:646–648.

30. Miklos, A. C., M. Sarkar, …, G. J. Pielak. 2011. Protein crowding tunes protein stability. *J. Am. Chem. Soc.* 133:7116–7120.

31. Benton, L. A., A. E. Smith, …, G. J. Pielak. 2012. Unexpected effects of macromolecular crowding on protein stability. *Biochemistry.* 51:9773–9775.

32. Hall, D., and A. P. Minton. 2003. Macromolecular crowding: qualitative and semiquantitative successes, quantitative challenges. *Biochim. Biophys. Acta.* 1649:127–139.

33. Wang, Q., A. Zhuravleva, and L. M. Gierasch. 2011. Exploring weak, transient protein—protein interactions in crowded in vivo environments by in-cell nuclear magnetic resonance spectroscopy. *Biochemistry.* 50:9225–9236.

34. Dhar, A., K. Girdhar, …, M. Gruebele. 2011. Protein stability and folding kinetics in the nucleus and endoplasmic reticulum of eucaryotic cells. *Biophys. J.* 101:421–430.

35. Dhar, A., A. Samiotakis, …, M. S. Cheung. 2010. Structure, function, and folding of phosphoglycerate kinase are strongly perturbed by macromolecular crowding. *Proc. Natl. Acad. Sci. USA.* 107:17586–17591.

36. Chen, E., A. Christiansen, …, P. Wittung-Stafshede. 2012. Effects of macromolecular crowding on burst phase kinetics of cytochrome *c* folding. *Biochemistry.* 51:9836–9845.

37. Li, C., Y. Wang, and G. J. Pielak. 2009. Translational and rotational diffusion of a small globular protein under crowded conditions. *J. Phys. Chem. B.* 113:13390–13392.

38. Wang, Y., C. Li, and G. J. Pielak. 2010. Effects of proteins on protein diffusion. *J. Am. Chem. Soc.* 132:9392–9397.

39. Pozdnyakova, I., J. Guidry, and P. Wittung-Stafshede. 2002. Studies of *Pseudomonas aeruginosa* azurin mutants: cavities in beta-barrel do not affect refolding speed. *Biophys. J.* 82:2645–2651.

40. Santoro, M. M., and D. W. Bolen. 1988. Unfolding free energy changes determined by the linear extrapolation method. 1. Unfolding of phenylmethanesulfonyl alpha-chymotrypsin using different denaturants. *Biochemistry.* 27:8063–8068.

41. Pace, C. N., and K. L. Shaw. 2000. Linear extrapolation method of analyzing solvent denaturation curves. *Proteins.* 41(*Suppl 4*):1–7.

42. Myers, J. K., C. N. Pace, and J. M. Scholtz. 1995. Denaturant m values and heat capacity changes: relation to changes in accessible surface areas of protein unfolding. *Protein Sci.* 4:2138–2148.

43. Engman, K. C., A. Sandberg, …, B. G. Karlsson. 2004. Probing the influence on folding behavior of structurally conserved core residues in P. aeruginosa apo-azurin. *Protein Sci.* 13:2706–2715.

44. Pozdnyakova, I., and P. Wittung-Stafshede. 2003. Approaching the speed limit for Greek Key beta-barrel formation: transition-state movement tunes folding rate of zinc-substituted azurin. *Biochim. Biophys. Acta.* 1651:1–4.

45. Pozdnyakova, I., and P. Wittung-Stafshede. 2001. Copper binding before polypeptide folding speeds up formation of active (holo) *Pseudomonas aeruginosa* azurin. *Biochemistry.* 40:13728–13733.

46. Wilson, C. J., and P. Wittung-Stafshede. 2005. Role of structural determinants in folding of the sandwich-like protein *Pseudomonas aeruginosa* azurin. *Proc. Natl. Acad. Sci. USA.* 102:3984–3987.

47. Wilson, C. J., D. Apiyo, and P. Wittung-Stafshede. 2006. Solvation of the folding-transition state in *Pseudomonas aeruginosa* azurin is modulated by metal: Solvation of azurin's folding nucleus. *Protein Sci.* 15:843–852.

48. Batra, J., K. Xu, and H. X. Zhou. 2009. Nonadditive effects of mixed crowding on protein stability. *Proteins.* 77:133–138.

49. Millett, I. S., S. Doniach, and K. W. Plaxco. 2002. Toward a taxonomy of the denatured state: small angle scattering studies of unfolded proteins. *Adv. Protein Chem.* 62:241–262.

50. Laurent, T. C., and J. Killander. 1964. Theory of gel filtration and its experimental verification. *J. Chromatogr.* 14:317–330.

51. Fodeke, A. A., and A. P. Minton. 2010. Quantitative characterization of polymer-polymer, protein-protein, and polymer-protein interaction via tracer sedimentation equilibrium. *J. Phys. Chem. B.* 114:10876–10880.

52. Hirai, M., S. Arai, …, T. Takizawa. 1998. Small-angle x-ray scattering and calorimetric studies of thermal conformational change of lysozyme depending on pH. *J. Phys. Chem. B.* 102:1308–1313.

53. Holthuis, J. C., and C. Ungermann. 2013. Cellular microcompartments constitute general suborganellar functional units in cells. *Biol. Chem.* 394:151–161.

54. Pozdnyakova, I., J. Guidry, and P. Wittung-Stafshede. 2001. Copper stabilizes azurin by decreasing the unfolding rate. *Arch. Biochem. Biophys.* 390:146–148.

55. Wilson, C. J., and P. Wittung-Stafshede. 2005. Snapshots of a dynamic folding nucleus in zinc-substituted *Pseudomonas aeruginosa* azurin. *Biochemistry.* 44:10054–10062.

56. Ai, X., Z. Zhou, …, W. Y. Choy. 2006. 15N NMR spin relaxation dispersion study of the molecular crowding effects on protein folding under native conditions. *J. Am. Chem. Soc.* 128:3916–3917.

57. Tjong, H., and H. X. Zhou. 2010. The folding transition-state ensemble of a four-helix bundle protein: helix propensity as a determinant and macromolecular crowding as a probe. *Biophys. J.* 98:2273–2280.

58. Zhou, H. X. 2013. Influence of crowded cellular environments on protein folding, binding, and oligomerization: biological consequences and potentials of atomistic modeling. *FEBS Lett.* 587:1053–1061.

59. Munishkina, L. A., A. Ahmad, …, V. N. Uversky. 2008. Guiding protein aggregation with macromolecular crowding. *Biochemistry.* 47:8993–9006.

60. Fuller, R. S., J. M. Kaguni, and A. Kornberg. 1981. Enzymatic replication of the origin of the *Escherichia coli* chromosome. *Proc. Natl. Acad. Sci. USA.* 78:7370–7374.

61. Phillip, Y., and G. Schreiber. 2013. Formation of protein complexes in crowded environments—from in vitro to in vivo. *FEBS Lett.* 587:1046–1052.

62. Christiansen, A., Q. Wang, …, P. Wittung-Stafshede. 2013. Effects of macromolecular crowding agents on protein folding in vitro and in silico. *Biophysical Reviews.* 5:137–145.

63. Walkiewicz, K., A. S. Benitez Cardenas, …, Y. Shamoo. 2012. Small changes in enzyme function can lead to surprisingly large fitness effects during adaptive evolution of antibiotic resistance. *Proc. Natl. Acad. Sci. USA.* 109:21408–21413.

64. Brandt, T., J. L. Kaar, …, D. B. Veprintsev. 2012. Stability of p53 homologs. *PLoS ONE.* 7:e47889.

65. Metcalfe, J., D. S. Dhindsa, …, A. Mourdjinis. 1969. Decreased affinity of blood for oxygen in patients with low-output heart failure. *Circ. Res.* 25:47–51.